

CHEMISTRY & SUSTAINABILITY

# CHEM **SUS** CHEM

ENERGY & MATERIALS

## Accepted Article

**Title:** Highly Efficient Gas Phase Oxidation of Renewable Furfural to Maleic Anhydride over Plate VPO Catalyst

**Authors:** Yugen Zhang, Xiukai Li, and Jogie Ko

This manuscript has been accepted after peer review and appears as an Accepted Article online prior to editing, proofing, and formal publication of the final Version of Record (VoR). This work is currently citable by using the Digital Object Identifier (DOI) given below. The VoR will be published online in Early View as soon as possible and may be different to this Accepted Article as a result of editing. Readers should obtain the VoR from the journal website shown below when it is published to ensure accuracy of information. The authors are responsible for the content of this Accepted Article.

**To be cited as:** *ChemSusChem* 10.1002/cssc.201701866

**Link to VoR:** <http://dx.doi.org/10.1002/cssc.201701866>

WILEY-VCH

[www.chemsuschem.org](http://www.chemsuschem.org)

A Journal of

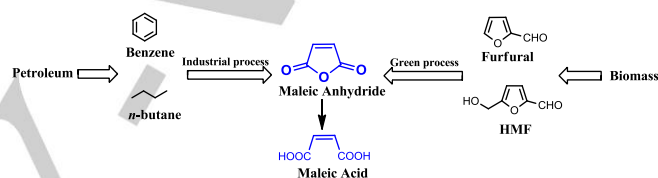


# Highly Efficient Gas Phase Oxidation of Renewable Furfural to Maleic Anhydride over Plate VPO Catalyst

Xiukai Li,<sup>[a]</sup> Jogie Ko<sup>[a]</sup> and Yugen Zhang\*<sup>[a]</sup>

**Abstract:** Maleic anhydride (MAh) and its acids are critical intermediates in chemical industry. The synthesis of maleic anhydride from renewable furfural is one of the most sought after processes in the field of sustainable chemistry. We report a plate vanadium phosphorous oxide (VPO) catalyst synthesized by a hydrothermal method with glucose as a green reducing agent for furfural oxidation to MAh in gas phase. The plate VPO<sub>HT</sub> catalyst has a preferentially exposed 200 crystal plane and exhibited dramatically enhanced activity, selectivity and stability as compared to conventional VPO catalysts and other state-of-the-art catalytic systems. At 360 °C reaction temperature with air as an oxidant, about 90% yield of MAh was achieved at 10 vol% of furfural in the feed, a furfural concentration value that is much higher than those (< 2 vol%) reported for other catalytic systems. The catalyst showed good long term stability and there was no decrease in activity and selectivity for MAh in the time-on-stream duration of 25 h. The high efficiency and catalyst stability established this system very prominent for the synthesis of maleic anhydride from renewable furfural.

product isolation, and better catalyst reutilization. There have been few reports on the gas phase fixed-bed catalytic oxidation of furfural to MAh<sup>[7]</sup>. However, current state-of-the-art systems are suffered from the low selectivity, low feed concentration (typically < 2 vol%) and low catalyst stability issues<sup>[7c]</sup>. For instance, VO<sub>x</sub>/Al<sub>2</sub>O<sub>3</sub> catalyst gave 73% of MAh yield at a furfural concentration of 1.6 vol% yet the long term stability of the catalyst was not clear<sup>[7c]</sup>. In light of the high demand for the synthesis of MAh from renewable resource, more catalytic processes merit to be explored for the potential practical application.



**Scheme 1.** Processes for the synthesis of maleic anhydride and maleic acid.

## Introduction

Maleic anhydride (MAh) and its acids (i.e., maleic acid and fumaric acid) are critical chemical intermediates used for the large volume production of lubricant additives, unsaturated polyester resins, vinyl copolymers, plasticizers, and pharmaceuticals<sup>[1]</sup>. Maleic anhydride is industrially manufactured from the gas phase oxidation of benzene and *n*-butane<sup>[2]</sup>. Further hydrolysis of maleic anhydride leads to maleic acid (MA). In view of renewable resources and chemical sustainability<sup>[1, 3]</sup>, biomass derived platform molecules such as furfural have been extensively studied as starting materials for the synthesis of maleic anhydride/acid<sup>[4]</sup>.

Various systems have been developed for the transformation of furfural to MAh/MA, generally with molecular oxygen or hydrogen peroxide as oxidants (Scheme 1). The homogeneous catalytic systems usually offer the desired product in less than 50% yields<sup>[4a-c, 5]</sup>. Heterogeneous catalytic systems (batch) could give higher yields of product, for examples, a titanium silicate-1 (TS-1) catalyst gave 78% yield of MA from furfural with H<sub>2</sub>O<sub>2</sub> (7.5 eq.) as an oxidant<sup>[4g]</sup> and a Mo-V-O catalyst gave 65% yield of MAh from furfural with pressurized O<sub>2</sub> (20 bar)<sup>[4h]</sup>. However, these catalysts suffered from critical stability issue as significant metal leaching was observed during the reaction. Besides the catalytic batch conversions, formic acid-mediated oxidation of furfural to MA with H<sub>2</sub>O<sub>2</sub> in a catalyst-free system has also been reported and 95% yield of MA was achieved<sup>[6]</sup>. The continuous flow gas phase reactions are important processes in chemical industry established by the many advantages such as higher operation temperature, easier

Vanadium phosphorous oxide (VPO) containing vanadyl pyrophosphate ((VO)<sub>2</sub>P<sub>2</sub>O<sub>7</sub>) as the main active phase is a well-known catalyst in *n*-butane oxidation to MAh, giving product yield of up to 90%<sup>[2, 8]</sup>. Previous mechanism studies have proposed that *n*-butane and furfural oxidation to MAh share the same furan-type intermediates<sup>[4h, 7c, 9]</sup>. We therefore envision that VPO-type catalysts might also be effective in the catalysis of furfural oxidation to MAh. However, there has been no open report on VPO catalyst for furfural oxidation in gas phase though various methods have been developed for the synthesis of VPOs<sup>[10]</sup>. In this work, we report a two-step hydrothermal method to synthesize plate VPO catalyst (VPO<sub>HT</sub>) by using glucose as a green reducing agent. The plate VPO<sub>HT</sub> catalyst was applied in the gas-phase oxidation of furfural to MAh and it exhibited dramatically enhanced activity, selectivity and stability. At 360 °C, about 90% yield of MAh was achieved at 10 vol% of furfural in the feed. The catalyst also demonstrated good long term stability and there was no decrease in activity for the duration of 25 h. This study provides a prominent catalytic system for the synthesis of maleic anhydride from renewable furfural.

[a] Dr. X. Li, Miss J. Ko and Dr. Y. Zhang  
Institute of Bioengineering and Nanotechnology, 31 Biopolis Way,  
The Nanos #04-01, Singapore 138669 (Singapore)  
Fax: (+65) 6478 9080  
Email: yg Zhang@ibn.a-star.edu.sg.

Supporting information for this article is given via a link at the end of the document.

## Results and Discussion

### Catalyst characterization

The preparation chemistry for the industrial VPO catalysts has long been a topic of research. VPO catalysts can be synthesized in either aqueous phase or organic (alcohol) phase. The VPO catalysts generated from the organic medium generally possess larger surface area and higher activities for *n*-butane oxidation than the catalysts generated from the aqueous medium. A major issue in the organic medium case is the use of large volumes of fatty alcohol and/or aromatic alcohol as reducing agent/solvent. There have also been reports on the successful hydrothermal synthesis of VPO catalysts starting from  $V_2O_4$  and  $H_3PO_4$ , or from  $V_2O_5$  and  $H_3PO_3$ , as the vanadium and phosphorus sources [11]. However,  $V_2O_4$  is an expensive reagent and  $H_3PO_3$  is highly toxic to handle. Herein, the  $VPO_{HT}$  catalyst was synthesized by using a modified hydrothermal method starting from inexpensive and easily available  $V_2O_5$  and  $H_3PO_4$  as starting materials and carbohydrate glucose as a green reducing agent. For comparison,  $VPO_{aq}$  and  $VPO_{org}$  catalysts have also been synthesized from respective aqueous and organic medium.

The structure and the morphology of the  $(VO)_2P_2O_7$  (VPO) catalysts are determined mainly by the precursor samples, viz.  $VOHPO_4 \cdot 0.5H_2O$  (VHPO). Figure 1 shows the SEM images of VPO samples prepared by different methods. The  $VPO_{aq}$  sample contains irregular particles (Figure 1a). The  $VPO_{org}$  sample contains agglomerated small plates with irregular particle sizes (Figure 1b). The  $VHPO_{HT}$  sample (precursor of  $VPO_{HT}$ ) from hydrothermal synthesis contains dispersed thin plates with smooth surface (Figure 1c). The  $VHPO_{HT}$  sample was dehydrated to  $VPO_{HT}$  in nitrogen gas at 400 °C for 12 h and its morphology was well retained as thin plates (Figure 1d). The  $VPO_{HT}$  plates have thickness of approximately 100 nm, and the particles are smooth and highly crystallized. BET surface area values of  $VPO_{aq}$ ,  $VPO_{org}$  and  $VPO_{HT}$  catalysts are 2.6, 20.1, and 9.7  $m^2 g^{-1}$ , respectively.

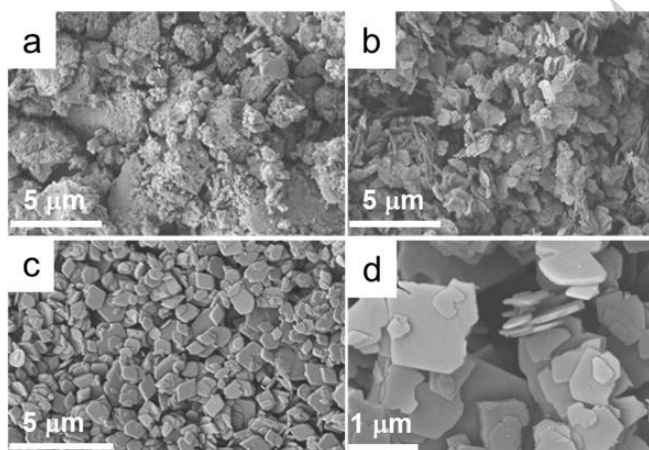


**Figure 1.** SEM images of (a) the  $VPO_{aq}$ ; (b)  $VPO_{org}$ ; (c)  $VHPO_{HT}$ ; (d)  $VPO_{HT}$ . All VPO catalysts were dehydrated from the corresponding precursors at 400 °C for 12 h in flowing  $N_2$ .

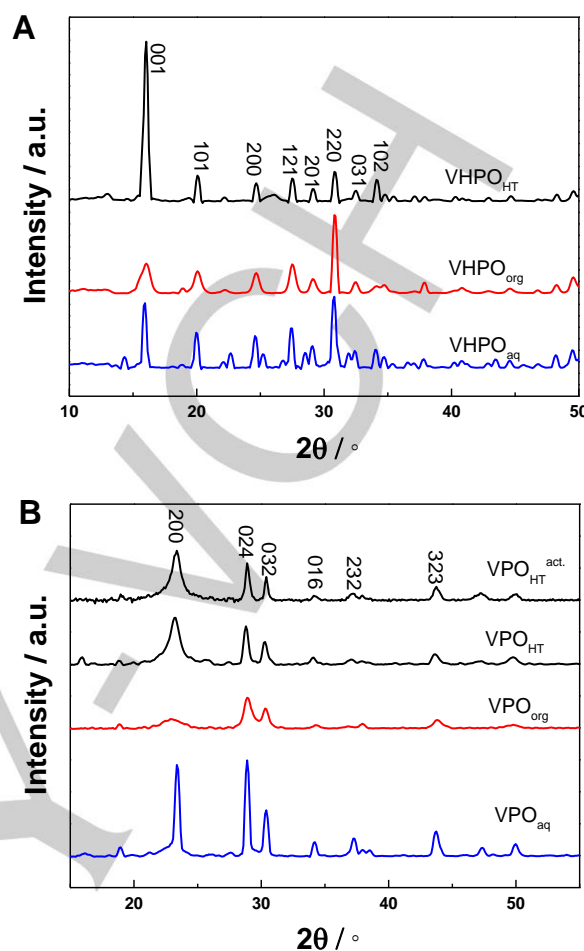


**Figure 2.** The XRD patterns of (A) the VHPO precursors synthesized by different methods, and (B) the VPO catalysts derived from the dehydration of VHPO precursors.  $VPO_{aq}$ ,  $VPO_{org}$  and  $VPO_{HT}$  catalysts were dehydrated from the corresponding precursors at 400 °C for 12 h in flowing  $N_2$ .  $VPO_{HT}^{act.}$  was the  $VPO_{HT}$  catalyst further activated in the reactant mixture (6% furfural in 10%  $O_2/He$ , 20  $mL min^{-1}$ ) at 340 °C for 8 h.

Figure 2 shows the XRD patterns of the VHPO precursors derived from different methods. All the samples exhibited the diffraction peaks assignable to crystalline  $VOHPO_4 \cdot 0.5H_2O$ . For the  $VHPO_{aq}$  and  $VHPO_{org}$  samples, the 220 peaks ( $2\theta = 30.8^\circ$ ) are more intense than the 001 peaks ( $2\theta = 16.1^\circ$ ). In contrast,  $VHPO_{HT}$  displays a much stronger 001 peak, indicating a different crystallinity or preferential growth of crystal faces. The 001 peak broadened the most significantly for  $VHPO_{org}$ . There have been reports that for VPO precursors synthesised in mixed alcohol solvent, the intercalation of organic molecules may result in structure disorder and the broadening of the 001 peak. [2b] Thus, the  $VHPO_{HT}$  from hydrothermal synthesis was better crystallized. After dehydration, the  $VPO_{HT}$  catalyst exhibits the highest relative intensity of the 200 peak to the 024 peak, indicating the 200 planes of the  $VPO_{HT}$  catalyst are well exposed. Such XRD features were retained for  $VPO_{HT}^{act.}$  which was further activated in the reactant mixture (6% furfural in 10%  $O_2/He$ , 20  $mL min^{-1}$ ) at 340 °C for 8 h. It is therefore deduced that the better crystallinity and the preferential growth of the 001

plane for the V<sub>HT</sub> precursor favours the exposure of the 200 plane of VPO [9b, 12]. It has been reported that 200 is the active face of VPO catalyst in *n*-butane oxidation to MANh [9a, 12a, b]. Thus, highly exposed 200 plane of VPO catalyst is an important character.

Vanadyl pyrophosphate ((V<sup>IV</sup>O)<sub>2</sub>P<sub>2</sub>O<sub>7</sub>) and vanadyl phosphate (V<sup>V</sup>OPO<sub>4</sub>) are the two major phases for vanadium phosphorous oxide (VPO) catalysts. The components of VPO catalyst are determined by both the precursor synthesis method and also the dehydration atmosphere. Raman spectroscopy is very sensitive to the small amount of V<sup>5+</sup> phases exist in those VPO samples (Figure 3). The signals at around ~930, ~1130, and ~1180 cm<sup>-1</sup> are the characteristics of the (VO)<sub>2</sub>P<sub>2</sub>O<sub>7</sub> phase, among them the signal at ~930 cm<sup>-1</sup> could be assigned to the ν<sub>as</sub>, P-O-P in the P<sub>2</sub>O<sub>7</sub><sup>2-</sup> unit [2, 13]. Various V<sup>5+</sup> phases coexist in the VPO<sub>aq</sub>, VPO<sub>org</sub>, and VPO<sub>HT</sub> samples, evidenced by the ~590, ~997, ~1017, ~1035, and ~1083 cm<sup>-1</sup> signals assignable to VOPO<sub>4</sub> phases including α-, β-, γ-VOPO<sub>4</sub> and VOPO<sub>4</sub>·2H<sub>2</sub>O [2, 12b, 14]. The V<sup>5+</sup> phases exist in larger proportion in the VPO<sub>HT</sub> sample that was activated in air. The additional signals at ~997 and ~1034 cm<sup>-1</sup> indicate the formation of more γ-VOPO<sub>4</sub> due to the oxidation in air. The Raman spectrum of the VPO<sub>HT</sub><sup>act.</sup> sample first activated in nitrogen then *in situ* treated in the reactant mixture (Figure 3e) differs remarkably to the spectrum of the sample activated only in nitrogen (Figure 3c). The V<sup>5+</sup> phases with Raman signal at ~1017 and ~1083 cm<sup>-1</sup> almost completely disappeared owing to the reduction by furfural.

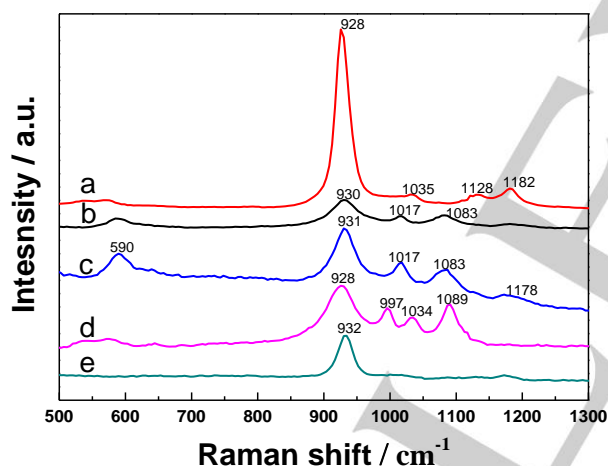


**Figure 3.** Raman spectra of the VPO catalysts derived from different methods. Samples: (a) VPO<sub>aq</sub>, N<sub>2</sub> activated at 400 °C for 12 h; (b) VPO<sub>org</sub>, activated in N<sub>2</sub> at 400 °C for 12 h; (c) VPO<sub>HT</sub>, activated in N<sub>2</sub> at 400 °C for 12 h; (d) VPO<sub>HT</sub><sup>air</sup>, activated in air at 400 °C for 12 h; (e) VPO<sub>HT</sub><sup>act.</sup>, activated in N<sub>2</sub> at 400 °C for 12 h, then further treated in the reactant mixture (6% furfural in 10% O<sub>2</sub>/He, 20 mL min<sup>-1</sup>) at 340 °C for 8 h.

Figure 4 depicts the temperature programmed reduction (TPR) behaviours of the VPO catalysts. All samples show one main reduction peak in the temperature range of 750–850 °C, attributable to the removal of the lattice oxygen in the VPO catalysts. The onset reduction temperature, which indicates the activity of lattice oxygen of VPO catalysts, are 777 °C for VPO<sub>aq</sub>, 740 °C for VPO<sub>org</sub>, 764 °C for VPO<sub>HT</sub>, and 767 °C for VPO<sub>HT</sub><sup>act.</sup>. The VPO<sub>aq</sub> sample showed the highest onset reduction temperature and consumed the least amount of hydrogen. Thus,

the lattice oxygen of VPO<sub>aq</sub> is the least active. The VPO<sub>HT</sub> and VPO<sub>HT</sub><sup>act.</sup> samples showed moderate reducibility among the four samples. Factors like phase composition, particle size, and crystal structure may affect the onset reduction temperature. It was evidenced by the Raman spectroscopy that V<sup>5+</sup> species related to VOPO<sub>4</sub> phases exist in some of the samples (Figure 3). Reduction of V<sup>5+</sup> to V<sup>4+</sup> species occurs at lower temperature and deeper reduction of V<sup>4+</sup> to V<sup>3+</sup> species occurs at higher temperature. The VPO<sub>org</sub> sample that possesses the smallest particle size and contains the VOPO<sub>4</sub> phases exhibited the lowest onset reduction temperature.

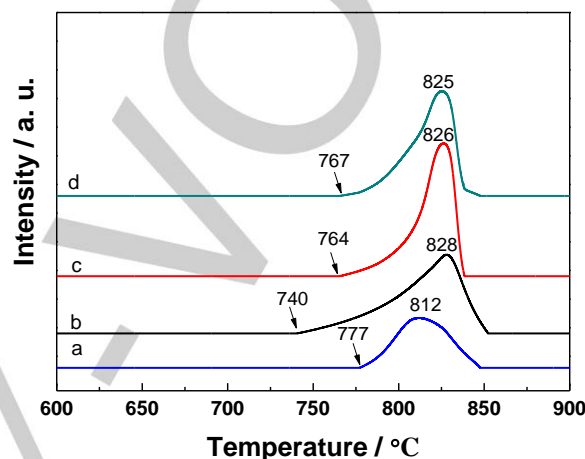


**Figure 4.** Temperature-programmed reduction (TPR) profiles of VPO catalysts (a) VPO<sub>aq</sub>, (b) VPO<sub>org</sub>, (c) VPO<sub>HT</sub>, and (d) VPO<sub>HT</sub><sup>act.</sup>. Catalysts were activated under the same conditions indicated in Figures 2&3.

#### Activity evaluation

For *n*-butane oxidation to MANh, it is recognized that crystalline (VO)<sub>2</sub>P<sub>2</sub>O<sub>7</sub> is the active phase while VOPO<sub>4</sub> is responsible for CO<sub>x</sub> formation [14-15]. However, for furfural oxidation reaction, the role of different phases of VPO remains unknown. Thus, various vanadium catalysts were evaluated for furfural oxidation, with the results shown in Table 1. At the reaction temperature of 340 °C, simple vanadium oxides (V<sub>2</sub>O<sub>5</sub> and V<sub>2</sub>O<sub>4</sub>) gave almost full furfural conversions, but the selectivities for CO<sub>x</sub> were around 80%. The selectivities for possible polymerized products were included in “others”. The V<sup>V</sup>OPO<sub>4</sub> catalyst showed relatively low activity (27.7% conversion) but good selectivity (87.4%) for MANh. 2-Furoic acid (FA) was detected as the main side product with 11.3% selectivity. The formation of CO<sub>x</sub> was insignificant (< 2% selectivity), and this is different to the case of *n*-butane oxidation over V<sup>V</sup>OPO<sub>4</sub> where CO<sub>x</sub> was the major side product [14-15]. The VPO<sub>aq</sub> catalyst with (V<sup>IV</sup>O)<sub>2</sub>P<sub>2</sub>O<sub>7</sub> as the major phase gave the lowest furfural conversion (18.5%) among VPOs probably owing to the smallest surface area value of 2.6 m<sup>2</sup> g<sup>-1</sup>. Maleic anhydride and 2-furoic acid was produced at the selectivities of 56.1% and 37.8%, respectively. The VPO<sub>org</sub> catalyst exhibited 60.4% furfural conversion and 79.8% selectivity toward MANh, while the selectivity for 2-furoic acid decreased to 8.2%. The VPO<sub>HT</sub> catalyst showed the best activity and selectivity among the three VPOs, with 80% furfural conversion and 95.3% selectivity for MANh. 2-Furoic acid was still observed yet at a

much lower selectivity of 1.6%. Although the VPO<sub>HT</sub> catalyst has an intermediate surface area value among the three VPOs, it showed the best catalytic performance. It is obvious that the catalyst activity is not only related to the total surface area but also the active surface area. The high catalytic activity of plate VPO<sub>HT</sub> should be related to its highly exposed 200 plane (Figure 2). This is also correlated to the results of temperature programmed reduction (TPR) analysis of the VPO catalysts (Figure 4). Though it seems that the lattice oxygen of VPO<sub>org</sub> is more reactive than VPO<sub>HT</sub>, VPO<sub>HT</sub> is practically more active for furfural oxidation which is due to its unique morphology and the preferentially exposed 200 plane.

The phase component of VPO catalyst is highly related to the conditions for catalyst precursor (viz. VOHPO<sub>4</sub>) dehydration and activation. Generally, the dehydration of VPO precursor in oxidizing atmosphere resulted in a catalyst with certain amount of V<sup>5+</sup> species [16]. In Table 1, when the VPO<sub>HT</sub> catalyst was dehydrated in air, the furfural conversion increased notably to 97.9% but the selective for MANh dropped to 86.7%, accompanied by the selectivity for CO<sub>x</sub> increased remarkably to 11.5%. When the VPO<sub>HT</sub> catalyst dehydrated in N<sub>2</sub> was further treated in the reactant mixture (6% furfural in 10% O<sub>2</sub>/He) at 340 °C for 8 h, it turned out that almost full furfural conversion and 97.9% selectivity for MANh was achieved. Thus, for a VPO<sub>HT</sub> that is freshly activated in N<sub>2</sub>, an initiation period is necessary to induce the suitable active sites/phases by removing the undesired V<sup>5+</sup> phases.

**Table 1.** Furfural gas phase oxidation over different phases of vanadium catalysts.

Catalyst	Conv. [%]	Sel. [%]			
		MANh	FA	Others	CO <sub>x</sub>
V <sub>2</sub> O <sub>5</sub>	98.8	17.5	0.0	4.0	78.6
V <sub>2</sub> O <sub>4</sub>	99.6	2.6	0.0	12.0	85.4
VOPO <sub>4</sub>	27.7	87.4	11.3	0.0	1.3
VPO <sub>aq</sub>	18.5	56.1	37.8	3.8	2.2
VPO <sub>org</sub>	60.4	79.8	8.2	7.9	4.2
VPO <sub>HT</sub>	80.0	95.3	1.6	2.5	0.6
VPO <sub>HT</sub> <sup>air</sup>	97.9	86.7	0.7	1.0	11.5
VPO <sub>HT</sub> <sup>act.</sup>	99.2	97.9	0.5	0.9	0.7

Reaction conditions: catalyst, 0.4 g; furfural concentration, 2 vol%; carrier gas, 10% O<sub>2</sub>/He, 20 mL min<sup>-1</sup>; reaction temperature, 340 °C. VPO<sub>aq</sub>, VPO<sub>org</sub> and VPO<sub>HT</sub>: dehydrated in N<sub>2</sub> at 400 °C for 12 h. VPO<sub>HT</sub><sup>air</sup>: dehydrated in air at 400 °C for 12 h. VPO<sub>HT</sub><sup>act.</sup>: first dehydrated in N<sub>2</sub> at 400 °C for 12 h, then treated in the reactant mixture (6% furfural 10% O<sub>2</sub>/He, 20 mL min<sup>-1</sup>) at 340 °C for 8 h. MANh: maleic anhydride; FA: 2-furoic acid; CO<sub>x</sub>: CO and CO<sub>2</sub>. "Others" include possible polymerized products and other unidentified products.

The catalyst performance is also influenced by the carrier gas for the reaction. The effect of oxygen concentration in the carrier gas was therefore studied (Figure 5). The furfural conversion generally increased with oxygen concentration in the carrier gas. An oxygen concentration around 10% is favourable for the best MANh selectivity of 98% at 340 °C. When synthetic air (21%O<sub>2</sub>/N<sub>2</sub>) was used as an oxidant, over 91% and 87% MANh selectivities were achieved at 340 °C and 360 °C, respectively. In view of the cost, air would be a better oxidant for practical application.

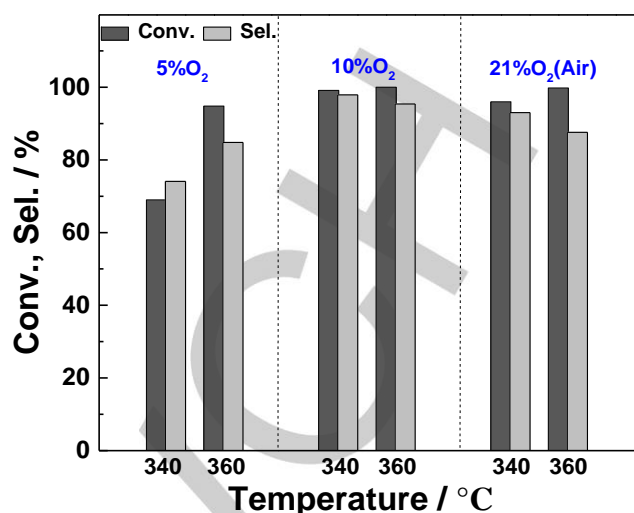


**Figure 5.** Furfural conversion and Manh selectivity over the VPO<sub>HT</sub><sup>act.</sup> catalyst with 5%, 10%, 21% oxygen in the carrier gas. Reaction conditions: VPO<sub>HT</sub><sup>act.</sup> catalyst, 0.4 g; carrier gas, 20 mL min<sup>-1</sup>; furfural concentration, 2 vol% in the feed.

In pursuit of a high output system, the present VPO<sub>HT</sub><sup>act.</sup> catalyst was evaluated at furfural concentrations of 2 vol%, 6 vol% and 10 vol% in the feed, with cheap synthetic air as the oxidant (Figure 6). At a reaction temperature below 360 °C, the furfural conversion decreased with its concentration in the feed. With the temperature rise, the furfural conversions increased and reached almost full at 360 °C (Figure 6A). With increasing reaction temperature, the selectivity for MANh also increased notably while the selectivity for 2-furoic acid decreased dramatically (Figure 6B). At the reaction temperature of 360 °C, the selectivities for MANh were 87.6%, 98.4%, and 90.8%, respectively, at furfural concentrations of 2 vol%, 6 vol% and 10 vol%. Thus, the present VPO<sub>HT</sub><sup>act.</sup> catalyst is efficient for the oxidation of furfural at the concentration up to 10 vol%, a value that is much higher than those (< 2 vol%) in literature reports. Further increase the furfural concentration in the feed would require higher reaction temperature or larger loading amount of catalyst.

The effect of the contact time was studied for 6 vol% furfural in the feed by changing the flow rate of the carrier gas (Figure 7A). At the flow rates of 20, 40, and 60 mL min<sup>-1</sup>, the contact time was 1.5, 0.75, and 0.5 seconds, respectively. At the reaction temperature of 340 °C, both the furfural conversion and Manh selectivity decreased linearly with the flow rate of the carrier gas, while the selectivity for 2-furoic acid increased. The conversion and selectivity can be further improved by increasing the reaction temperature when the contact time was short (or higher flow rate of the carrier gas). It is shown in Figure 7B, 92.8% conversion of furfural and 94.4% selectivity for MANh could be achieved at 360 °C for the reaction carried out at furfural concentration of 6 vol% and a flow rate of 60 mL min<sup>-1</sup> (GHSV: 7200 h<sup>-1</sup>). When the reaction temperature exceeded 360 °C, the selectivity for CO<sub>x</sub> increased and the selectivity for MANh dropped accordingly.

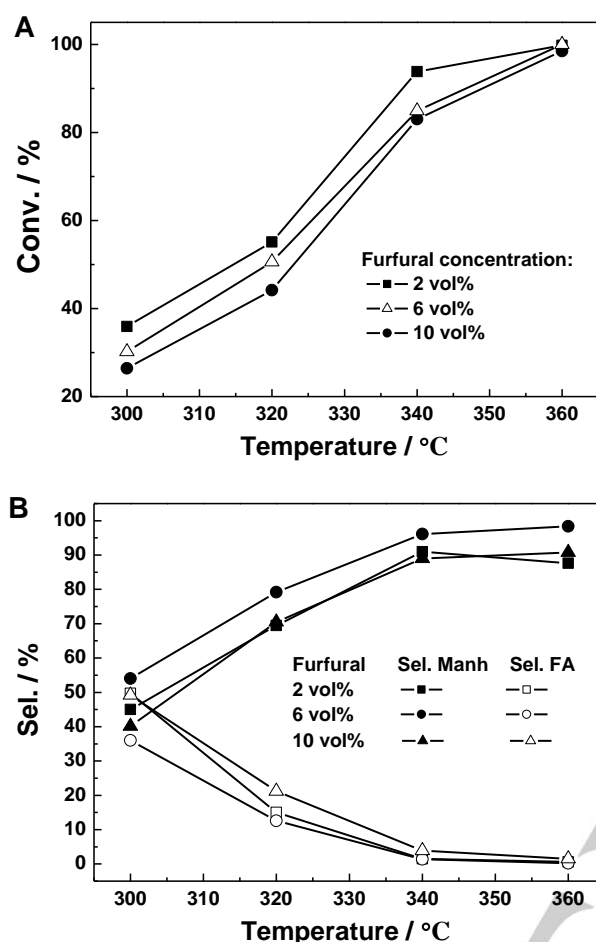
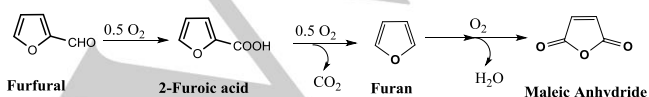


**Figure 6.** (A) Furfural conversion and (B) MANh and FA selectivities as a function of reaction temperature at 2%, 6%, and 10 vol% furfural concentrations in the feed. Reaction conditions:  $\text{VPO}_{\text{HT}}^{\text{act}}$  catalyst, 0.4 g; carrier gas, synthetic air (21%  $\text{O}_2/\text{N}_2$ ), 20  $\text{mL min}^{-1}$ . MANh: maleic anhydride; FA: 2-furoic acid.

From Figures 6B and 7B, it is seen that 2-furoic acid was the major side product for furfural oxidation over the  $\text{VPO}_{\text{HT}}$  catalyst. With temperature rise, the selectivities for 2-furoic acid decreased while the selectivity for Manh increased accordingly, suggesting that 2-furoic acid is a key intermediate in the current reaction and that Manh was derived from the consecutive oxidation of 2-furoic acid. On the basis of product distribution, the reaction pathway for furfural oxidation to Manh with VPO catalyst was proposed (Scheme 2), which is also consistent with previous reported mechanism study<sup>[4h, 7c, 17]</sup>. Because furan was detected in very trace amount or was not detected, we propose that the oxidation of furfural to 2-furoic acid is the rate-determining step for furfural oxidation over the  $\text{VPO}_{\text{HT}}$  catalysts, while the decarboxylation of 2-furoic acid to furan and the subsequent oxidation of furan to Manh are fast.



**Scheme 2.** The proposed reaction pathway for furfural oxidation to maleic anhydride with VPO catalysts.

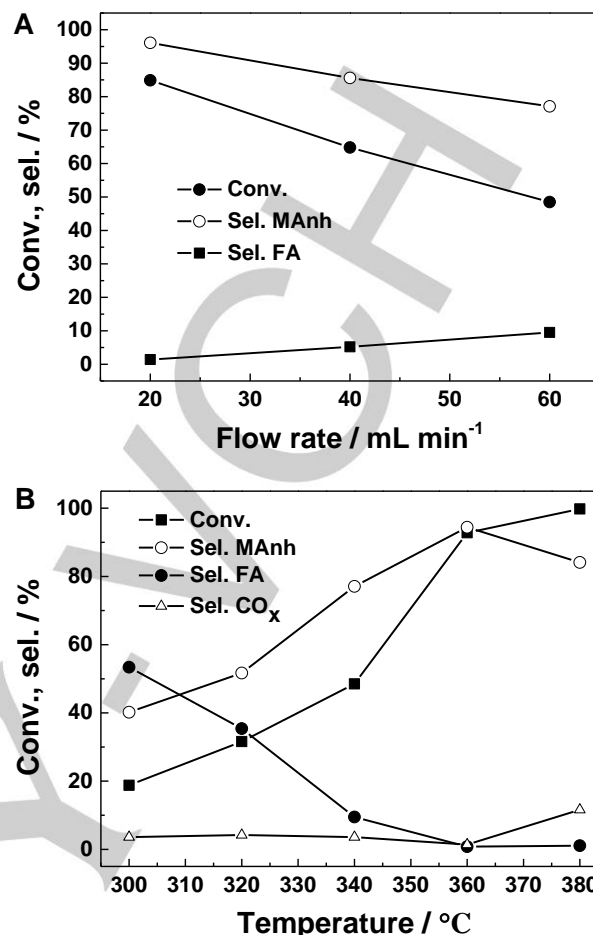


**Figure 7.** (A) Furfural conversion and MANh/FA selectivities at the carrier gas of 20, 40, and 60  $\text{mL min}^{-1}$  and the reaction temperature of 340 °C, and (B) temperature dependence of furfural oxidation at carrier gas of 60  $\text{mL min}^{-1}$  (GHSV: 7200  $\text{h}^{-1}$ ). Other reaction conditions:  $\text{VPO}_{\text{HT}}^{\text{act}}$  catalyst, 0.4 g; furfural concentration, 6 vol% in feed; carrier gas, 21%  $\text{O}_2/\text{N}_2$ .

The stability of the  $\text{VPO}_{\text{HT}}$  catalyst was tested as a function of time on stream at 6 vol% of furfural concentration and a flow rate of 40  $\text{mL min}^{-1}$  (GHSV: 4800  $\text{h}^{-1}$ ). As shown in Figure 8, the initial conversion and Manh selectivity were 92.9% and 94.5%, respectively. Furfural conversion increased gradually to 99% in the first 7 hours, indicating an initiation period for the *in situ* activation of  $\text{VPO}_{\text{HT}}$ . Within the duration of 25 hours, the catalyst was stable and there was no appreciable decrease in activity and selectivity for MANh. The MANh product was collected as white solid from the outlet of the reactor by simple condensation in air (Supporting Information, Figure S1). NMR analysis confirmed that the collected MANh was in high purity (Supporting Information, Figure S2). XRD analysis for the used catalyst indicates that the structure of the catalyst was intact after activity testing (Supporting Information, Figure S3). The used catalyst was also subjected to thermogravimetric analysis (TGA) (Supporting Information, Figure S4). The weight loss in the temperature range of 300–500 °C was less than 2%, indicating the coke deposition on sample surface is insignificant. The superb stability enables the  $\text{VPO}_{\text{HT}}$  catalyst a prominent one for furfural oxidation to MANh.

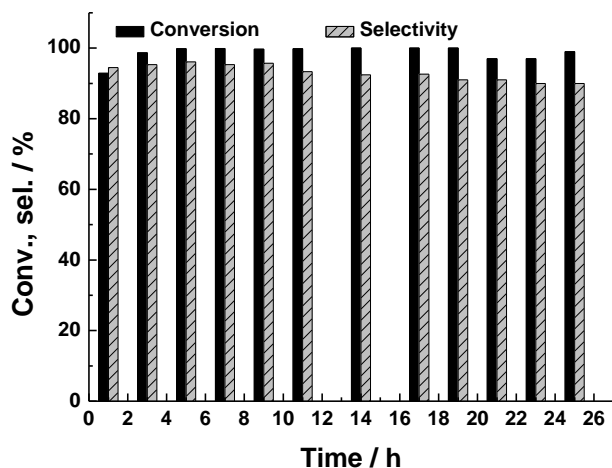


**Figure 8.** Time on stream test for furfural oxidation to MAAnh over the VPO<sub>HT</sub> catalyst. Reaction conditions: catalyst, 0.4 g; furfural concentration, 6 vol%; carrier gas, 21% O<sub>2</sub>/N<sub>2</sub>, 40 mL min<sup>-1</sup> (GHSV: 4800 h<sup>-1</sup>), 350 °C.

## Conclusions

We demonstrate here a plate vanadium phosphorous oxide (VPO) as efficient catalysts for furfural oxidation to maleic anhydride in gas phase. The present VPO<sub>HT</sub> catalyst synthesized by a hydrothermal method with glucose as a green reducing agent has novel plate morphology, preferentially exposed 200 crystal plane which played key role in the catalytic reaction, and exhibited superb catalytic performance as compared to other state-of-the-art catalytic systems. About 90% yield of MAAnh was achieved at furfural concentration of 10 vol% and air as an oxidant. MAAnh can be collected as high purity solid by simple air condensation. The catalyst showed good stability and there was no decrease in activity and selectivity in the duration of 25 h on time stream. The high efficiency and catalyst stability established this system very prominent for the synthesis of maleic anhydride from renewable furfural.

## Experimental Section

### VPO<sub>HT</sub> catalyst preparation

The VPO<sub>HT</sub> catalyst was synthesized by a two-step hydrothermal method in a Teflon-lined autoclave. Firstly, a mixture of V<sub>2</sub>O<sub>5</sub> (2.73 g), glucose (0.81 g), and water (90 mL) was heated at 180 °C for 12 h in the autoclave. After the autoclave was cooled to room temperature, the black solid (V<sub>2</sub>O<sub>4</sub>) was separated by filtration, washed twice with water, and then dried at 100 °C overnight. In the second step, the mixture of V<sub>2</sub>O<sub>4</sub> (0.83 g), H<sub>3</sub>PO<sub>4</sub> (85%, 0.82 mL), PEG (0.5 g), and water (30 mL) was heated in the autoclave at 160 °C for 24 h. The blue product was collected by filtration, washed with ethanol and water, and then dried at 100 °C overnight. The catalyst precursor was dehydrated at 400 °C for 12 h in flowing N<sub>2</sub> (100 mL min<sup>-1</sup>) to generate the VPO<sub>HT</sub> catalyst.

### Catalyst evaluation

Catalytic performances of catalysts (typically 0.4 g, 35–60 mesh) for the gas phase oxidation of furfural to maleic anhydride was evaluated in a quartz fixed-bed microreactor ( $\Phi = 6$  mm) with a continuous reactant down flow. All catalysts were pressed into pellets and then crushed and sieved to 35–60 mesh before activity evaluation. Furfural was charged in a saturator that was submerged in an oil bath, and it was brought to the reactor by the bubbles of carrier gas (10%O<sub>2</sub>/He or synthetic air, flow rate 20–60 mL min<sup>-1</sup>). The concentration of furfural in the gas phase was controlled by the temperature of the oil bath. On-line gas chromatography (Shimadzu GC2014) equipped with FID and TCD was used to analyse the outlet effluent after the system was stabilized for 1 h at each temperature point. A capillary column (HP FFAP, 30 m × 0.32 mm, 0.25  $\mu$ m) was used to separate the organic components, and a packed carbon column (3 mm × 300 mm) was used to separate CO and CO<sub>2</sub>.

### Characterization techniques

Powder X-ray Diffraction (XRD) was conducted using a Bruker automatic diffractometer (Bruker D8 discover GADDS) with monochromatized Cu-K $\alpha$  radiation ( $\lambda = 0.15406$  nm) at a setting of 30 kV.

The BET surface areas and pore structures were measured by Micromeritics ASAP 2020. The samples were degassed at 250 °C for 3 h before N<sub>2</sub> adsorption. The SEM images were obtained with a JEOL JSM 7500 scanning electron microscope.

Temperature-programmed reduction (TPR) was carried out in the temperature range of 100–800 °C. The sample (50 mg) was reduced in a feed of 5% H<sub>2</sub>/Ar (30 mL min<sup>-1</sup>) at a heating rate of 5 °C min<sup>-1</sup>.

Raman analysis was conducted using Horiba Jobin Yvon Modular Raman Spectrometer. The laser excitation wavelength: Stellar Pro Argon-ion laser at 514 nm (Green). Laser power used: 50 mW. The Raman system was calibrated using a silicon reference before the measurement.

## Acknowledgements

This work was supported by the Institute of Bioengineering and Nanotechnology (Biomedical Research Council, Agency for Science, Technology and Research (A\*STAR), Singapore), Biomass-to-Chemicals Program (Science and Engineering Research Council, A\*STAR, Singapore).

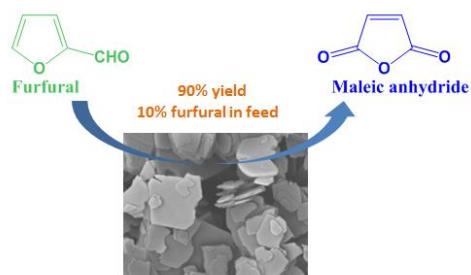
**Keywords:** biomass • furfural • VPO catalyst • maleic anhydride • selective oxidation

- [1] R. Wojcieszak, F. Santarelli, S. Paul, F. Dumeignil, F. Cavani, R. V. Gonçalves, *Sustain. Chem. Process.* **2015**, *3*, 1–11.
- [2] a) X. K. Li, W. J. Ji, J. Zhao, Z. Zhang, C. T. Au, *Appl. Catal. a-Gen.* **2006**, *306*, 8–16; b) X. K. Li, W. J. Ji, J. Zhao, Z. B. Zhang, C. T. Au, *J. Catal.* **2006**, *238*, 232–241.
- [3] a) M. Besson, P. Gallezot, C. Pinel, *Chem. Rev.* **2014**, *114*, 1827–1870; b) J. van Haveren, E. L. Scott, J. Sanders, *Biofuels Bioprod. Bioref.* **2008**, *2*, 41–57; c) D. M. Alonso, J. Q. Bond, J. A. Dumesic, *Green Chem.* **2010**, *12*, 1493–1513; d) M. Stocker, *Angew. Chem. Int. Ed.* **2008**, *47*, 9200–9211; e) D. M. Alonso, S. G. Wettstein, J. A. Dumesic, *Chem. Soc. Rev.* **2012**, *41*, 8075–8098; f) D. P. Ho, N. Huu Hao, W. Guo, *Bioresour. Technol.* **2014**, *169*, 742–749; g) R. A. Sheldon, *Green Chem.* **2014**, *16*, 950–963.
- [4] a) J. Lan, Z. Chen, J. Lin, G. Yin, *Green Chem.* **2014**, *16*, 4351–4358; b) S. Shi, H. Guo, G. Yin, *Catal. Commun.* **2011**, *12*, 731–733; c) H. Guo, G.

- Yin, *J. Phys. Chem. C* **2011**, *115*, 17516–17522; d) Z. Du, J. Ma, F. Wang, J. Liu, J. Xu, *Green Chem.* **2011**, *13*, 554-557; e) S. Li, K. Su, Z. Li, B. Cheng, *Green Chem.* **2016**, *18*, 2122-2128; f) S. Shi, H. Guo, G. Yin, *Catal. Commun.* **2011**, *12*, 731-733; g) X. Li, B. Ho, Y. Zhang, *Green Chem.* **2016**, *18*, 2976-2980; h) N. Alonso-Fagundez, I. Agirrezabal-Telleria, P. L. Arias, J. L. G. Fierro, R. Mariscal, M. Lopez Granados, *Rsc Adv.* **2014**, *4*, 54960-54972; i) J. Lan, J. Lin, Z. Chen, G. Yin, *Acs Catal.* **2015**, *5*, 2035-2041; j) M. Krystof, M. Pérez-Sánchez, P. Domínguez de María, *ChemSusChem* **2013**, *6*, 826-830; k) X. Li, X. Lan, T. Wang, *Catal. Today* **2016**, *276*, 97-104.
- [5] a) H. Choudhary, S. Nishimura, K. Ebitani, *Appl. Catal. a-Gen.* **2013**, *458*; b) N. Alonso-Fagundez, V. Laserna, A. C. Alba-Rubio, M. Mengibar, A. Heras, R. Mariscal, M. L. Granados, *Catal. Today* **2014**, *234*, 285-294; c) H. Choudhary, S. Nishimura, K. Ebitani, *Chem. Lett.* **2012**, *41*, 409-411; d) S. Peleteiro, S. Rivas, J. Luis Alonso, V. Santos, J. Carlos Parajo, *Bioresource Technol.* **2016**, *202*, 181-191.
- [6] X. Li, B. Ho, D. S. W. Lim, Y. Zhang, *Green Chem.* **2017**, *19*, 914-918.
- [7] a) W. V. Sessions, *J. Am. Chem. Soc.* **1928**, *50*, 1696-1698; b) M. S. Murthy, K. Rajamani, *Chem. Eng. Sci.* **1974**, *29*, 601-609; c) N. Alonso-Fagundez, M. Lopez Granados, R. Mariscal, M. Ojeda, *ChemSusChem* **2012**, *5*, 1984-1990; d) E. R. Nielsen, *Ind. Eng. Chem.* **1949**, *41*, 365-368.
- [8] a) G. Centi, F. Trifiro, J. R. Ebner, V. M. Franchetti, *Chem. Rev.* **1988**, *88*, 55-80; b) J. C. Volta, *Comptes Rendus De L Academie Des Sciences Serie Ii Fascicule C-Chimie* **2000**, *3*, 717-723.
- [9] a) B. Chen, E. J. Munson, *J. Am. Chem. Soc.* **2002**, *124*, 1638-1652; b) G. Centi, F. Trifiro, *Chem. Eng. Sci.* **1990**, *45*, 2589-2596.
- [10] a) L. M. Cornaglia, C. A. Sanchez, E. A. Lombardo, *Appl. Catal. a-Gen.* **1993**, *95*, 117-130; b) G. J. Hutchings, R. Higgins, *Appl. Catal. a-Gen.* **1997**, *154*, 103-115; c) E. A. Lombardo, C. A. Sanchez, L. M. Cornaglia, *Catal. Today* **1992**, *15*, 407-418.
- [11] a) J. A. Lopez-Sanchez, L. Griesel, J. K. Bartley, R. P. K. Wells, A. Liskowski, D. S. Su, R. Schlogl, J. C. Volta, G. J. Hutchings, *Phys. Chem. Chem. Phys.* **2003**, *5*, 3525-3533; b) J. A. Lopez-Sanchez, J. K. Bartley, R. P. K. Wells, C. Rhodes, G. J. Hutchings, *New J. Chem.* **2002**, *26*, 1613-1618; c) J. K. Bartley, J. A. Lopez-Sanchez, G. J. Hutchings, *Catal. Today* **2003**, *81*, 197-203.
- [12] a) B. GrzybowskaSwierkosz, *Appl. Catal. a-Gen.* **1997**, *157*, 409-420; b) G. Busca, F. Cavani, G. Centi, F. Trifiro, *J. Catal.* **1986**, *99*, 400-414; c) M. Havecker, R. W. Mayer, A. Knop-Gericke, H. Bluhm, E. Kleimenov, A. Liskowski, D. Su, R. Follath, F. G. Requejo, D. F. Ogletree, M. Salmeron, J. A. Lopez-Sanchez, J. K. Bartley, G. J. Hutchings, R. Schlogl, *J. Phys. Chem. B* **2003**, *107*, 4587-4596.
- [13] Z. Q. Zhou, H. Y. Xu, W. J. Ji, Y. Chen, *Catal. Lett.* **2004**, *96*, 221-226.
- [14] V. V. Gulians, J. B. Benziger, S. Sundaresan, I. E. Wachs, J. M. Jehng, J. E. Roberts, *Catal. Today* **1996**, *28*, 275-295.
- [15] a) B. Schiott, K. A. Jorgensen, R. Hoffmann, *J. Phys. Chem.* **1991**, *95*, 2297-2307; b) J. Ziolkowski, E. Bordes, P. Courtine, *J. Mol. Catal.* **1993**, *84*, 307-326.
- [16] a) M. Abon, J. M. Herrmann, J. C. Volta, *Catal. Today* **2001**, *71*, 121-128; b) F. Cavani, S. Ligi, T. Monti, F. Pierelli, F. Trifiro, S. Albonetti, G. Mazzoni, *Catal. Today* **2000**, *61*, 203-210.
- [17] a) N. A. Milas, W. L. Walsh, *J. Am. Chem. Soc.* **1935**, *57*, 1389-1393; b) W. Zhang, Y. L. Zhu, S. Niu, Y. W. Li, *J. Mol. Catal. a-Chem.* **2011**, *335*, 71-81.

## Entry for the Table of Contents

A plate VPO<sub>HT</sub> catalyst synthesized by a hydrothermal method has preferentially exposed 200 crystal planes and exhibited excellent activity and selectivity for furfural oxidation to maleic anhydride.



*Xiukai Li, Jogie Ko and Yugen Zhang\**

**Highly Efficient Gas Phase Oxidation of Renewable Furfural to Maleic Anhydride over Plate VPO Catalyst**